

# VIRTUAL SLIT FOR IMPROVED RESOLUTION IN LONGITUDINAL EMITTANCE MEASUREMENT \*

K. Ruisard<sup>†</sup>, A. Aleksandrov, A. Shishlo  
 Oak Ridge National Laboratory, Oak Ridge, TN, USA

## Abstract

A technique to reduce point-spread originating from physical slit width in emittance measurements is described. This technique is developed to improve phase resolution in a longitudinal emittance apparatus consisting of a dipole magnet, energy-selecting slit and bunch shape monitor. In this apparatus, the energy and phase resolutions are directly proportional to the width of the slit. The virtual slit method allows sub-slit resolution, with penalty in measurement time and dynamic range. The bunch phase profile is measured at two points in the energy distribution with a separation less than the physical slit width. The difference of these two profiles is used to reconstruct the profile from a virtual slit of width equal to that separation.

## INTRODUCTION

Accurate measurement of beam phase space distributions is crucial for verifying correct operation and understanding accelerator dynamics. Phase space measurement can both be the source for simulation bunches and the basis for benchmarks of accelerator models. Longitudinal parameters in particular reflect dynamics within accelerating structures. Work at the Beam Test Facility (BTF) at the Spallation Neutron Source (SNS) has focused on detailed characterization of the beam distribution, including high-dimensional measurements [1] and development of high-dynamic range diagnostics capable of halo measurement [2]. The goal of this work is to obtain loss-level accuracy with particle-in-cell simulation, where the simulation results can be verified down to the halo level.

The phase space measurements use a slit-scan technique, where each dimension is isolated by masking the beam with a thin slits. While the bunch shape monitor (BSM) has sufficient resolution to image the bunch phase distribution, finite slit widths upstream of the BSM cause significant point spread in the BSM. A virtual slit technique is developed to reduce the point spread effect in the phase measurement, significantly improving the resolution of the phase measurement without modifying the existing hardware.

This paper first describes the apparatus for measurement of the longitudinal phase space at the BTF. The virtual slit

\* This manuscript has been authored by UT-Battelle, LLC, under Contract No. DE-AC05-00OR22725 with the U.S. Department of Energy. The United States Government retains, and the publisher, by accepting the article for publication, acknowledges that the United States Government retains a non-exclusive, paid-up, irrevocable, world-wide license to publish or reproduce the published form of this manuscript, or allow others to do so, for United States Government purposes. The Department of Energy will provide public access to these results of federally sponsored research in accordance with the DOE Public Access Plan.

<sup>†</sup> ruisardkj@ornl.gov

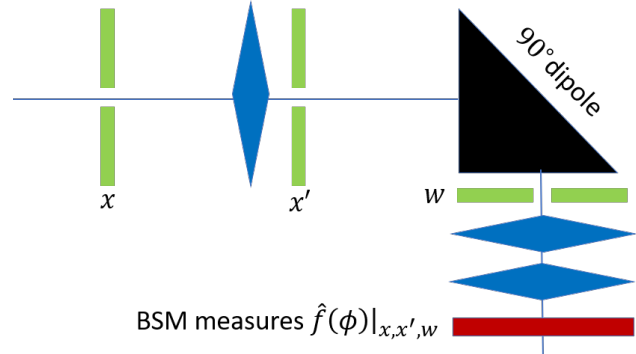


Figure 1: Diagram of longitudinal emittance apparatus. The notation  $\hat{f}(\phi)|_{x,x',w}$  is used to indicate that the BSM measures the phase profile for the fraction of the beam that passes through the upstream  $x$ ,  $x'$  and  $w$  slits.

technique is introduced for a wide-aperture slit, with an example measurement provided by PIC simulation of the setup. The case of a narrow slit aperture, with reduced but still significant point spread error, is also discussed. The use of a narrow slit complicates the virtual slit approach, but a solution is described. Finally, the data from virtual slit measurements is used to estimate the width of the physical slit aperture.

## APPARATUS

The BTF is a test-stand experiment designed as a clone of the SNS front-end, including  $H^-$  ion source, LEPT, RFQ and four MEBT quadrupoles, as well as a MEBT extension enabling extensive phase space diagnostics and transport studies. A detailed description of the facility can be found in [3].

The apparatus for measurement of the longitudinal phase space is situated in the 2.5 MeV MEBT. The device consists of a  $90^\circ$  dipole and energy-selecting slit followed by the BSM. The BSM measures the phase profile for the selected energy. The longitudinal phase space  $f(\phi, w)$  is measured by scanning the energy selection. Figure 1 shows the geometry of the emittance measurement. Two vertical slits upstream of the dipole are used to create a beam with small horizontal spread at the dipole entrance. In total there are three vertical slits, indicated by green rectangles. Additionally, three quadrupoles (indicated by blue diamonds) are used to control beam size on the energy slit and at the BSM.

At the energy slit location, two different widths are available: 200  $\mu\text{m}$  and 1 mm. In this document, they will be

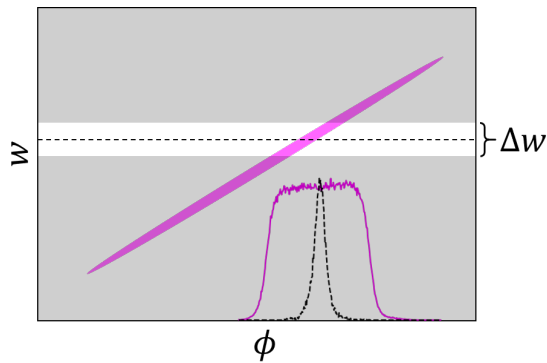


Figure 2: Illustration of longitudinal phase space at the BSM location. The unshaded window represents the portion of beam that passes through a 1 mm energy slit. Due to the high correlation, the projected rms phase width of that beamlet (solid magenta curve) is significantly wider than that of an infinitely thin slice (dashed black).

colloquially referred to as the “narrow” and “wide” slits. After manufacturing, a Phosphor coating is deposited on the slit to enable dual-use as a profile monitor. This deposition is not well-controlled and acts to reduce the width of the slit from the design value. While this is a relatively small error for the wide slit, it measurably affects the width of the narrow slit.

The largest source of error in the emittance apparatus is point spread in the phase measurement, which originates as a result of the width of energy slit and the large linear correlation between phase and energy. The BSM is 4.2 meters downstream of the RFQ exit. Between the RFQ and the BSM, the bunch expands longitudinally and the longitudinal phase space becomes highly correlated as illustrated in Fig. 2. The energy slit makes a selection that is much narrower than the total energy spread in the beam. For the narrow 200 μm slit,  $\Delta w \sim 2$  keV compared to rms width 24 keV [4]. Therefore, the point-spread effect on the energy profile is relatively small.

However, the spread in energy is correlated with a spread of arrival phase at the BSM. As depicted in Fig. 2, the projected phase profile of the energy slice  $\Delta w$  is wider than the true phase profile of an infinitely thin slice. The size of this error is much larger relative to the beam width. The rms point spread estimated in [4] is  $3.3^\circ$  compared the expected phase width of  $6^\circ$ . In other words, the phase width of the beam is very near the resolution limits of the emittance apparatus.

For the wide 1 mm slit,  $\Delta w \sim 10$  keV. Therefore, the point-spread effect from the slit width is very large in both the phase and energy dimensions.

## VIRTUAL SLIT TECHNIQUE

The virtual slit technique reduces the effect of point spread by effectively reducing the slit width without the need for physically modifying the slit. A virtual slit is generated by combining two phase profile measurements that are sepa-

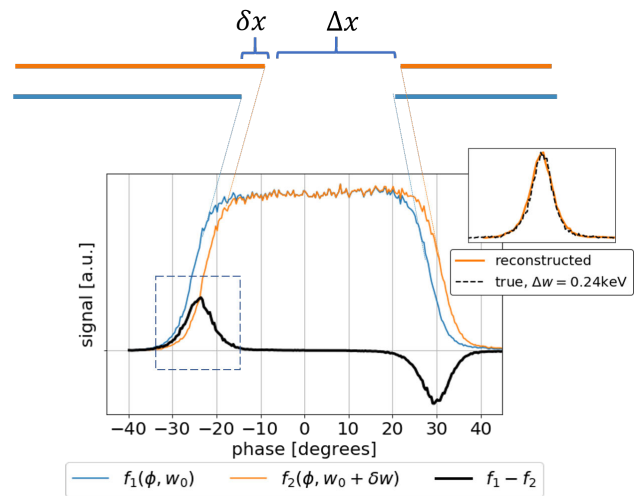


Figure 3: Illustration of virtual slit concept using wide (1 mm) slit. The orange and blue profiles are the phase profile measured with the BSM for two differentially-separated energies, illustrated here as a offset in slit location  $\delta x$ . The black curve is the difference profile, and the region in the dashed outline is the reconstructed phase profile.

rated by a small step in energy, where the energy step is smaller than the range that passes through the slit. It is easiest to consider moving the energy slit by a small step  $\delta x$ , where  $\delta x < \Delta x$  where  $\Delta x$  is the physical slit width. The two waveforms are subtracted and, as shown, their difference has two peaks: one positive and one negative. Each peak is the phase profile corresponding to the narrow energy band  $\delta w$  of the edge region, where the effective width of the virtual slit is  $\delta x$ . This process is illustrated in Fig. 3 using parameters for the wide slit.

This technique is analogous to the measurement of beam profiles using scrapers. In this system, a transverse profile can be measured by scanning a scraper across the beam in  $\hat{x}$  and recording the transmitted current. The measured curve is the cumulative function  $I(x) = \int_{-\infty}^x f(\hat{x})d\hat{x}$  that is differentiated to reconstruct the profile  $f(x)$ . The change  $\delta I$  for step size  $\delta x$  is proportional to the current that would be measured by a slit of width  $\delta x$ . In the case of the virtual slit, the change of the measured phase profile with incremental energy step,  $\delta f(\phi)$ , is the profile for a slice of phase space with width equal to the energy step  $\delta w$ .

The profiles shown in Fig. 3 were obtained via simulation of the emittance apparatus. The PIC code PyORBIT is used [5]. A bunch created by self-consistent simulation of the BTF RFQ is propagated to the plane of the energy slit. Slit apertures are applied at the location of the three vertical slits, with width equal to the slit design width (either 200 μm or 1 mm). Multiple simulations are run for various positions of the third (energy) slit, and for each the macroparticle coordinates are saved at the BSM location. For the plot shown, a virtual slit width of  $\delta x = 0.05$  mm is used.

Simulation enables comparison between the “true” phase width (the width of a very thin energy slice) with the profile

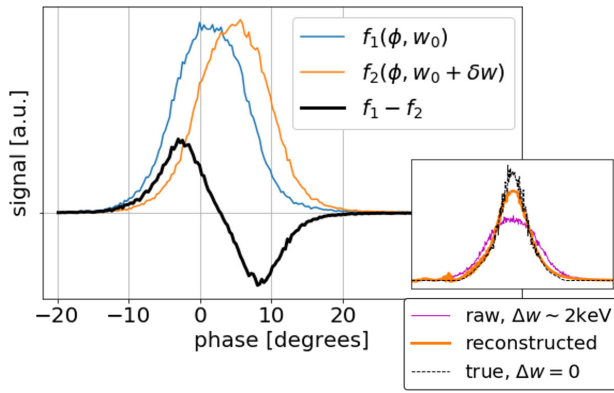


Figure 4: Illustration of virtual slit concept using narrow (0.2 mm) slit. The orange and blue profiles are the phase profile for a small step  $\delta w$ , the black curve is the difference profile. The inset plot compares the raw “measured” phase profile, which includes energy spread from finite slit size, to the reconstructed and true phase profiles.

obtained through the virtual slit technique. The inset plot in Fig. 3 shows this comparison: the true and reconstructed profiles are nearly identical. In this simulation case, the rms width with a 1% threshold is  $3.9^\circ$  for both the virtual slit profile and the thin slice.

### Reconstruction of Narrow Slit Profiles

The point spread effect of the narrow slit is a much smaller effect for the narrow,  $200\ \mu\text{m}$  slit. However, the point spread error is still the dominant effect in emittance measurements, as discussed in [4]. In the simulation case, for a thin energy slice  $\Delta w = 0.2\ \text{keV}$  the 100% rms phase width is  $4.2^\circ$ . However, the phase measured with realistic slit apertures was  $5.2^\circ$ . Even with the narrow slit, the point spread effect leads to  $\sim 20\%$  overestimation of the measured phase width.

The virtual slit reconstruction can be applied to narrow slit profiles, but there is an extra complication, as illustrated in Fig. 4. Unlike the case with the wide slit, the two difference profiles are not well-separated. It is possible to untangle the profiles if it can be assumed that they are identical except for translation.

Let the true phase profile be  $G(\phi)$  and let the black curve in Fig. 4 be called  $g(\phi)$ .  $g(\phi)$  can be expressed as

$$g(\phi) = G(\phi) - G(\phi + \Phi) \quad (1)$$

where  $\Phi$  is the translation along  $\hat{\phi}$ . The virtual slit subtraction should deliver two profiles whose centers are separated by a distance proportional to the width of the physical slit. Therefore,  $\Phi \propto \Delta x$  for slit width  $\Delta x$ . For a measured difference profile, the separation between peaks can be used to calculate the physical slit width, which is discussed below.

$G(\phi)$  can be reconstructed from the measured  $g(\phi)$  by

$$G(\phi) = \sum_{k=0}^{\infty} g(\phi + k\Phi). \quad (2)$$

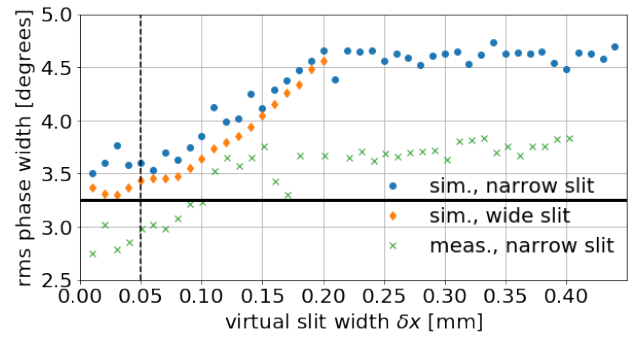


Figure 5: Dependence of reconstructed phase width on size of virtual slit. A 5% threshold is applied.

The assumption that the phase profiles are identical except for translation is valid. In general, the phase profile varies slowly with energy and for a small step  $\delta w \sim 0.5\ \text{keV}$  ( $\delta x \sim 0.05\ \text{mm}$ ) they should be nearly identical. Any inconsistencies are expected to be artifact from particle noise or response of viewscreen in the BSM.

The result of applying the reconstruction in Eq. (2) can be seen in the inset in Fig. 4. It is apparent that the reconstructed profile (solid orange curve) is significantly narrower than the raw curve (solid magenta), which is the uncorrected phase profile, but still wider than the “true” phase width (dashed black). For a threshold of 5%, the raw rms phase width is  $4.7^\circ$  and the reconstructed width is  $3.6^\circ$ . This is still slightly larger than the true width of  $3.2^\circ$ , but the point spread error is reduced.

This extra step in the reconstruction can introduce additional artifact due to imperfect cancellation of the peak and anti-peak waveforms. This can be mitigated by applying the summation in both directions and combining the two reconstructed profiles, or by applying a higher threshold.

### Optimal Width of Virtual Slit

The virtual slit should be significantly narrower than the physical slit in order to reduce point spread error. In practice the limit arises due to decreasing signal-noise ratio, which applies to both virtual and physical slits. In simulation this noise originates from granularity of the macroparticle distribution.

In both simulation and measurement, a virtual slit width  $\leq 0.05\ \text{mm}$  was optimal. The dependence of the reconstructed profile width is shown in Fig. 5. For virtual slit widths larger than the physical slit, the rms width flattens and is equal to the width of the “raw” profile without reconstruction. In both simulation and measurement, as the virtual width is reduced the reconstructed profile saturates at or below  $0.05\ \text{mm}$ . While the wide slit case reaches the “true” profile width (horizontal line) in simulation, the narrow slit reconstruction is less effective and there is still residual error. This limitation is likely related to the extra step in reconstruction (Eq. (2)).

Content from this work may be used under the terms of the CC BY 3.0 licence (© 2020). Any distribution of this work must maintain attribution to the author(s), title of the work, publisher, and DOI

### Measurement of Narrow Slit Width

As mentioned, the virtual slit technique can also be applied to measure the physical width of a slit. This is most useful for the narrow slit, where the contribution of the Phosphor layer depth is relatively large. This complements previous efforts to measure slit width, which include direct optical examination of a spare determined to have a width of  $0.17 \pm 0.01$  mm. Measurement of the installed slit is preferred, which requires an in-situ technique. Two methods were previously applied: (1)  $0.27 \pm 0.09$  from imaging of the slit illuminated by beam and (2)  $0.17 \pm .01$  by measuring the ratio of current transmitted by the wide and narrow slits.

As a third method, the slit width can be determined by looking at the distance between peak and anti-peak in the differential waveform  $f_1 - f_2$ . This distance, measured in BSM phase, can be transformed to transverse position at the slit with knowledge of the dispersion and linear  $\phi - w$  correlation. When the spacing between the two slit positions ( $\delta x$ ) is wider than the physical slit ( $\Delta x$ ), the phase separation between peaks is linear in  $\delta x$ . However, when  $\delta x < \Delta x$ , the distance between peaks becomes fixed and is proportional to the slit width  $\Delta x$ . This can be expressed as:

$$\Delta\phi = \begin{cases} \Delta x \frac{d\phi}{dx} & \text{if } \delta x < \Delta x \\ \delta x \frac{d\phi}{dx} & \text{if } \delta x \geq \Delta x \end{cases} \quad (3)$$

Both the slit width  $\Delta x$  and the transformation  $d\phi/dx$  can be determined by fitting Eq. (3) to measurements at different virtual slit spacings. This is illustrated in simulation in Fig. 6, where the slit width is known and is exactly 0.2 mm. A least-squares fit gives  $\Delta x = 0.205 \pm 0.002$  mm and  $d\phi/dx = 54.0 \pm 0.2$  degrees/mm. Errorbars are derived from fit uncertainty.

A fit to measured data is shown in Fig. 7. In this case, the fitted parameters are  $\Delta x = 0.155 \pm 0.002$  mm and  $d\phi/dx = 57.2 \pm 0.4$  degrees/mm, errorbars again are due only to fit uncertainty. The  $d\phi/dx$  parameter can be independently calculated from calibration data:  $d\phi/dx = 58.6 \pm 1.0$  degrees/mm. Based on the agreement of the  $d\phi/dx$  parameter, we judge the measured width  $\Delta x$  to be reliable. However, this is noticeably narrower than previous measurements which requires further investigation.

### SUMMARY

This paper discussed implementation of a virtual slit technique to improve phase resolution in a longitudinal emittance device. The technique is more broadly applicable to slit-based imaging devices where sub-slit resolution is desired. As demonstrated via simulation, the virtual slit technique can be deployed to enable appropriate phase resolution even in the case of a very wide slit. In the case of a narrow slit, the point spread error on the rms phase can be reduced although not completely eliminated. The virtual slit correction to the narrow slit data is less straightforward than in the wide slit case, requiring an extra step to separate two overlapping phase profiles.

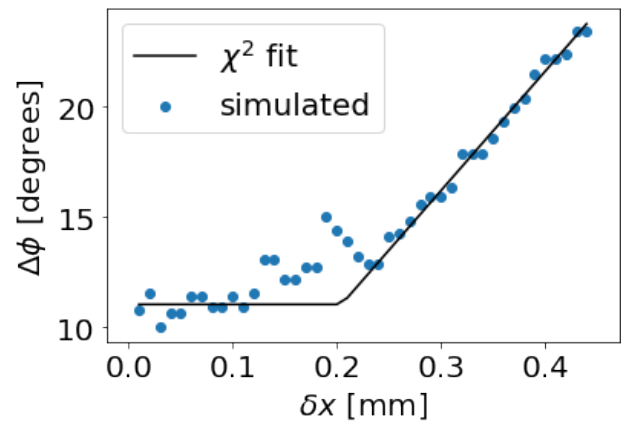


Figure 6: Least squares fit to determine narrow slit width using profiles from simulation with known slit width 0.2 mm.

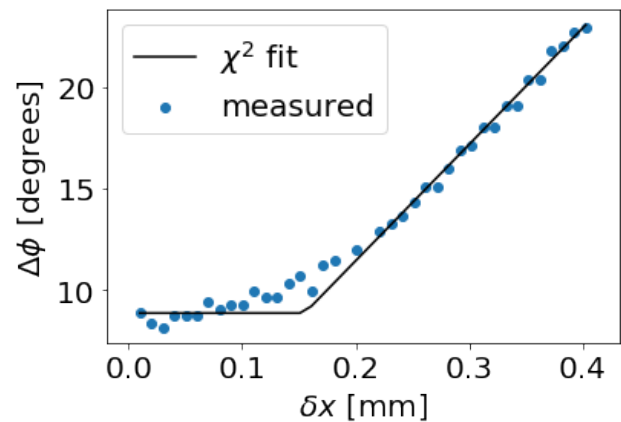


Figure 7: Least squares fit for measured profiles from virtual slit method with narrow slit.

This technique was implemented as an alternative to deconvolution of the point spread function. Deconvolution of measured and simulated signals was attempted, but the method was too sensitive to noise to provide useful results. The virtual slit was less sensitive to noise, although there was a penalty on signal-to-noise ratio similar to the penalty for using a physically narrower slit.

Despite the costs, the virtual slit is a convenient method for improving measurement resolution without modification of hardware, or vacuum breaks. Compared to a physical slit, a continuum of virtual slit sizes is available. This flexibility allows measurement of the physical slit width.

### ACKNOWLEDGEMENTS

This research used resources at the Spallation Neutron Source, a DOE Office of Science User Facility operated by the Oak Ridge National Laboratory.

### REFERENCES

- [1] B. Cathey, S. Cousineau, A. Aleksandrov and A. Zhukov, "First Six Dimensional Phase Space Measurement of an Accelerator"

- Beam”, *Phys. Rev. Lett.*, vol. 121, no. 6, p. 064804, 2018. doi:10.1103/PhysRevLett.121.064804
- [2] A. Aleksandrov, in preparation.
- [3] Z. Zhang, S. Cousineau, A. Aleksandrov, A. Menshov, and A. Zhukov, “Design and commissioning of the Beam Test Facility at the Spallation Neutron Source”, *Nuclear Instruments and Methods in Physics Research A*, vol. 949, p. 162826, 2020. doi:10.1016/j.nima.2019.162826
- [4] K. Ruisard, A. Aleksandrov, S. Cousineau, A. Shishlo, V. Zoganis and A. Zhukov, “High dimensional characterization of the longitudinal phase space formed in a radio frequency quadrupole”. arXiv:2008.06565
- [5] A. Shishlo, S. Cousineau, J. Holmes, and T. Gorlov, “The Particle Accelerator Simulation Code PyORBIT”, *Procedia Computer Science*, vol. 51, pp. 1272–1281, 2015. doi:10.1016/j.procs.2015.05.312